JOURNAL OF SOLID STATE CHEMISTRY 115, 476–483 (1995)

Structural Relations in Mixed Oxides $Cu_xZn_{1-x}Nb_2O_6$

J. Norwig, H. Weitzel, H. Paulus, G. Lautenschläger, J. Rodriguez-Carvajal,† and H. Fuess

Fachgebiet Strukturforschung, Fachbereich Materialwissenschaft, TH Darmstadt, Petersenstrasse 20, D-64287 Darmstadt, Germany; and †Laboratoire Léon Brillouin, (CEA-CNRS), CE de Saclay, F-91191, Gif sur Yvette, Cedex, France

Received May 16, 1994; accepted July 28, 1994

DEDICATED TO PROFESSOR HEINZ-DIETER LUTZ ON THE OCCASION OF HIS 60TH BIRTHDAY

Crystal structures of monoclinic $CuNb_2O_6$ and mixed niobates $Cu_xZn_{1-x}Nb_2O_6$, with $x = 0.85$ and 0.36, respectively, have been solved by neutron powder and X-ray single-crystal diffraction. Space groups and cell dimensions are $P2_1/c$, $a = 5.0064(1)$ Å, $b = 14.1733(3)$ Å, $c = 5.7615(1)$ Å, $\beta = 91.672(1)°$ for monoclinic $CuNb_2O_6$; $P2_1/c$, $a = 5.0070(1)$ Å, $b = 14.1706(2)$ Å, $c = 5.7547(1)$ Å, and $\beta = 91.451(1)°$ for $Cu_{0.85}Zn_{0.15}Nb_2O_6$; and $Pbcn$, $a = 14.187(5)$ Å, $b = 5.730(2)$ Å, and $c = 5.031(2)$ Å for $Cu_{0.36}Zn_{0.64}Nb_2O_6$. The crystal structure of orthorhombic $CuNb_2O_6$ was confirmed by neutron powder and X-ray single-crystal diffraction. The orientations of the O–Cu–O axes, elongated due to Jahn–Teller distortion, differ in a characteristic way for orthorhombic $CuNb_2O_6$ on one hand and monoclinic $CuNb_2O_6$ and the monoclinic mixed oxides on the other hand. For $Cu_{0.36}Zn_{0.64}Nb_2O_6$ no elongated axes were found by diffraction methods. A thermally or stress-induced, irreversible transformation from monoclinic to orthorhombic $CuNb_2O_6$ has been observed.

I. INTRODUCTION

The crystal structure of the mineral columbite, (Fe, Mn)Nb_2O_6, was determined by X-ray diffraction (1). Isomorphism of niobates MNb_2O_6 (M = Mn, Fe, Co, Ni) and $MnTa_2O_6$ was reported based on profile analysis of neutron powder diffraction patterns (2). This structure type can be derived from a hexagonal closed packing of oxygen ions. Half of the oxygen octahedra are occupied by metal ions forming zigzag chains of edge-sharing MO_6 octahedra. These parallel zigzag chains build up layers with the same metal ion M, which are stacked up in an order M–Nb–Nb–M–Nb–Nb–M.

Contradictory results were reported for $CuNb_2O_6$: An orthorhombic modification (3), a monoclinic distorted columbite structure (4), and the existence of both phases (5) were described. Whereas modification with columbite structure was definitely excluded (6), the existence of columbite-type $CuNb_2O_6$ was confirmed by a structure refinement of a neutron powder diffraction pattern (7). The obtained Cu–O distances of 242 pm (2×), 198 pm (2×), and 197 pm (2×) reveal the usual Jahn–Teller distortion of a Cu(II) coordination sphere. The existence of the monoclinic modificatiòn has not been proven by a structure determination up to now.

Besides the discussion on the existence and the crystal structures of the two modifications of $CuNb_2O_6$, another remarkable aspect is observed for mixed oxides $Cu_xZn_{1-x}Nb_2O_6$ ($0 \le x \le 1$). In the range $0.4 < x < 0.9$, the lattices are distorted to monoclinic unit cells, and for $0.9 \le x < 1$, a miscibility gap to $CuNb_2O_6$ is postulated (6). $ZnNb_2O_6$ and compounds with $0 < x \le 0.4$ crystallize like $CuNb_2O_6$ in an orthorhombic columbite-type structure (6, 8). The surprising conclusion from previous work is therefore that some mixed oxides are monoclinic, although both end members of this system have the same orthorhombic symmetry. In order to elucidate structural relationships in mixed niobates $Cu_xZn_{1-x}Nb_2O_6$, the crystal structures of some compounds belonging to this system are studied in this work. Some preliminary results have already been published in a short communication (9).

II. EXPERIMENTAL DETAILS

1. Preparations

All samples were prepared from high-purity agents, most of them distributed by Aldrich: Cu_2O (97%), CuO (99.9+%), HNO_3 (65%) (puriss., Merck Darmstadt), Nb_2O_5 (99.99%), and ZnO (99.9%). Crucibles of platinum or platinum/iridium were used for melts, and for subsolidus reactions crucibles of alumina.

Copper zinc niobates $Cu_xZn_{1-x}Nb_2O_6$, with $x = 0.1, 0.2, \ldots, 0.9$ and 0.85, 0.925, 0.95, 0.975 and orthorhombic $CuNb_2O_6$ were synthesized as powders by mixing stoichiometric amounts of CuO, ZnO, and Nb_2O_5. The mixtures were ground thoroughly in a ball mill and pressed to pellets with a pressure of 400–700 MPa. The pellets were annealed in a muffle furnace for 7 days at 850°C in air. To ensure complete reaction of the agents, the pellets were reground, pressed, and annealed again under the same

0022-4596/95 $6.00

TABLE 1
Experimental Setups of Single-Crystal X-Ray Diffraction Experiments on Orthorhombic $CuNb_2O_6$ and $Cu_{0.36}Zn_{0.64}Nb_2O_6$

	Substance	
	$CuNb_2O_6$	$Cu_{0.36}Zn_{0.64}Nb_2O_6$
Color	Black	Transmission: light green Reflection: black
Size	0.075 × 0.09 × 0.14 mm³	0.12 × 0.16 × 0.6 mm³
Faces	1 0 0 0.045 mm² −1 0 0 0.045 mm² 0 1 0 0.070 mm² 0 −1 0 0.070 mm² 0 0 1 0.038 mm² 0 0 −1 0.038 mm²	1 0 0 0.057 mm² −1 0 0 0.057 mm² 0 1 0 0.080 mm² 0 −1 0 0.080 mm² 0 0 1 0.286 mm² 0 0 −1 0.286 mm²
Radiation	Mo$K\alpha$, 0.71073 Å	Mo$K\alpha$, 0.71073 Å
Monochromator	Graphite	Graphite
Mode of scan	$2\theta/\omega = 1/1$, "learned profile"	$2\theta/\omega = 1/1$, "learned profile"
Scan range	$3° < 2\theta < 70°$ $0 \leq h \leq 22$ $0 \leq k \leq 8$ $0 \leq l \leq 8$	$3° < 2\theta < 70°$ $-22 \leq h \leq 22$ $-9 \leq k \leq 0$ $0 \leq l \leq 8$
Reflections measured	3149	1775
Unique reflections	897	900
Lattice constants	a = 14.097(6) Å b = 5.613(2) Å c = 5.123(2) Å	a = 14.187(5) Å b = 5.730(2) Å c = 5.031(2) Å
Linear absorption coefficient	104 cm⁻¹	108 cm⁻¹
Absorption correction	Numerical, 1120 grid points	Numerical, 3072 grid points
R_{int}	2.54%	3.23%
Structure determination	Directly refined with SHELX-76 (*10*); for initial parameters see (*7*)	Direct methods (SHELXS-86 (*11*)); refinement with SHELX-76 (*10*)
R^a	2.98%	3.04%
$R_w{}^a$	2.19%	3.18%
$R_g{}^a$	2.10%	3.55%
$R_m{}^a$	2.10%	3.55%
w^a	$2.3805/(\Sigma\,|F|)^2$	$9.0597/(\Sigma\,|F|)^2$

[a] For definition of the residuals see (*10*).

conditions. The color of the products changed according to their copper content from colorless zinc niobate to light greenish yellow to the olive-green orthorhombic copper niobate. In the range $0.85 < x < 1$, no single-phase products were obtained. Monoclinic $CuNb_2O_6$ was prepared as a dark, greenish-brown powder by oxidation of $CuNbO_3$ (5). The simultaneously formed CuO was removed by aqueous nitric acid (HNO_3 (65%): 4 H_2O).

In order to grow single crystals of $CuNb_2O_6$, a melt of formerly monoclinic $CuNb_2O_6$ was cooled from 1200°C at 3°C/min in oxygen atmosphere. The experiment yielded some black orthorhombic crystals with volumes of up to 10^{-3} mm³. After the separation of appropriate crystals, the sample was ground. X-ray powder diffraction confirmed the single-phase nature of this sample.

A single crystal of $Cu_{0.36}Zn_{0.64}Nb_2O_6$ was synthesized when a mixture of the oxides with the stoichiometry $Cu_{0.5}Zn_{0.5}Nb_2O_6$ decomposed. The sample was molten in a tube of Pt/Ir, heated up to a maximal 1500°C. The product consisted of transparent light-green and dark-red crystals. As the color and shape of the green crystals resembled the crystals of orthorhombic $CuNb_2O_6$, one of them was chosen for structural studies. A refinement of the Cu/Zn site occupation converged to $x = 0.36(8)$ in $Cu_xZn_{1-x}Nb_2O_6$.

2. *Structure Determination and Refinement*

X-ray data collection on the two orthorhombic compounds, $CuNb_2O_6$ and $Cu_{0.36}Zn_{0.64}Nb_2O_6$, was performed on a STOE-Stadi-4 diffractometer. Experimental data are listed in Table 1.[1] Neutron powder diffraction patterns of monoclinic and orthorhombic $CuNb_2O_6$ and of mono-

[1] Auxiliary material is deposited at CSD-#: 57567, Fachinformationszentrum Energie, Physik, Mathematik GmbH, D-76344 Eggenstein-Leopoldshafen, Germany.

clinic $Cu_{0.85}Zn_{0.15}Nb_2O_6$ were recorded at LLB, Saclay, and ILL, Grenoble, respectively. Structural parameters were refined with the program LHPM1 (12), which is based on DBW3.2 by Wiles and Young (13) and applies the full pattern least-squares profile analysis method described by Rietveld (14). Pseudo-Voigt profile functions were fitted using the profile function

$$G_{ik} = \gamma \frac{c_0^{1/2}}{H_k \pi (1 + c_0 x_{ik}^2)} + (1 - \gamma) \frac{c_1^{1/2}}{H_k \pi^{1/2}} \exp(-c_1 x_{ik}), \quad [1]$$

where

$$\gamma = \gamma_1 + \gamma_2 2\theta + \gamma_3 (2\theta)^2 \quad [2]$$

is the peak shape function, and

$$H_k = (u \tan^2\theta + v \tan\theta + w)^{1/2} \quad [3]$$

is the full-width at half-maximum, with $c_0 = 4$, $c_1 = 4 \ln 2$, $x_{ik} = (2\theta_i - 2\theta_k)/H_k$, and k labels the kth Bragg reflection.

Peak asymmetry was approximated with an equation given by Howard (15) which uses sums of five pseudo-Voigt profiles to describe single Bragg reflections. In Table 2,[1] information about the experimental setups and the refined nonstructural parameters are listed. In Figs. 1a–1c, plots of observed and calculated powder diffraction data and their differences are given.

3. Thermal Analysis

The thermal behavior of orthorhombic and monoclinic $CuNb_2O_6$ was investigated with a Setaram TG-DTA 92, performing simultaneously difference thermoanalysis and thermogravimetry. The samples were heated and cooled in crucibles of platinum in an oxygen atmosphere with rates of 3, 5, or 10°C per minute. Temperatures ranged from room temperature to 1200°C.

III. RESULTS AND DISCUSSION

1. Crystal Structures

Atomic coordinates and isotropic temperature factors of monoclinic $CuNb_2O_6$, refined from neutron powder data in space group $P2_1/c$, are given in Table 3.[1] Anisotropic refinement of the temperature factors yields a significantly increased parameter β_{22} of Cu. An attempt to explain this high value by a reduced symmetry, i.e., space groups $P2_1$ or $P\bar{1}$, results in better Bragg R residuals, but also in highly correlated coordinates of atoms, which are on symmetry-equivalent positions in $P2_1/c$. The refinements with reduced symmetry ($P2_1$, $P\bar{1}$) con-

TABLE 2
Experimental Setups, Refined Global Parameters, and Lattice Constants of Neutron Powder Diffraction Experiments with Monoclinic $CuNb_2O_6$ and $Cu_{0.85}Zn_{0.15}Nb_2O_6$

	Substance	
	$CuNb_2O_6$	$Cu_{0.85}Zn_{0.15}Nb_2O_6$
Diffractometer	D1A at LLB, Saclay	D2B at ILL, Grenoble
Wavelength	1.9845 Å	1.594 Å
$2\theta_{min}$, stepwidth, $2\theta_{max}$	7.50°, 0.05°, 149.95°	10.00°, 0.05°, 157.00°
Space group	$P2_1/c$	$P2_1/c$
Lattice constants	a = 5.0064(1) Å	a = 5.0070(1) Å
	b = 14.1733(3) Å	b = 14.1706(2) Å
	c = 5.7615(1) Å	c = 5.7547(1) Å
	β = 91.672(1)°	β = 91.451(1)°
Halfwidth parameters (see Eq. [3])	u = 0.098(7)	u = 0.067(3)
	v = −0.229(14)	v = −0.148(6)
	w = 0.340(7)	w = 0.224(3)
Profile parameters (see Eq. [2])	γ_1 = 0.18(4)	γ_1 = 0.21(3)
	γ_2 = −0.002(1)	γ_2 = −0.0049(8)
	γ_3 = 0.000044(7)	γ_3 = 0.000045(5)
Asymmetry parameter	P = 0.252(6)	P = 0.044(4)
R_p[a]	3.68%	4.07%
R_{wp}[a]	4.51%	5.21%
χ^2[a]	2,77	10.00
Durbin–Watson d[a]	0.41	0.35
Bragg R[a]	2.79%	3.19%

[a] For definition of the residuals see (12).

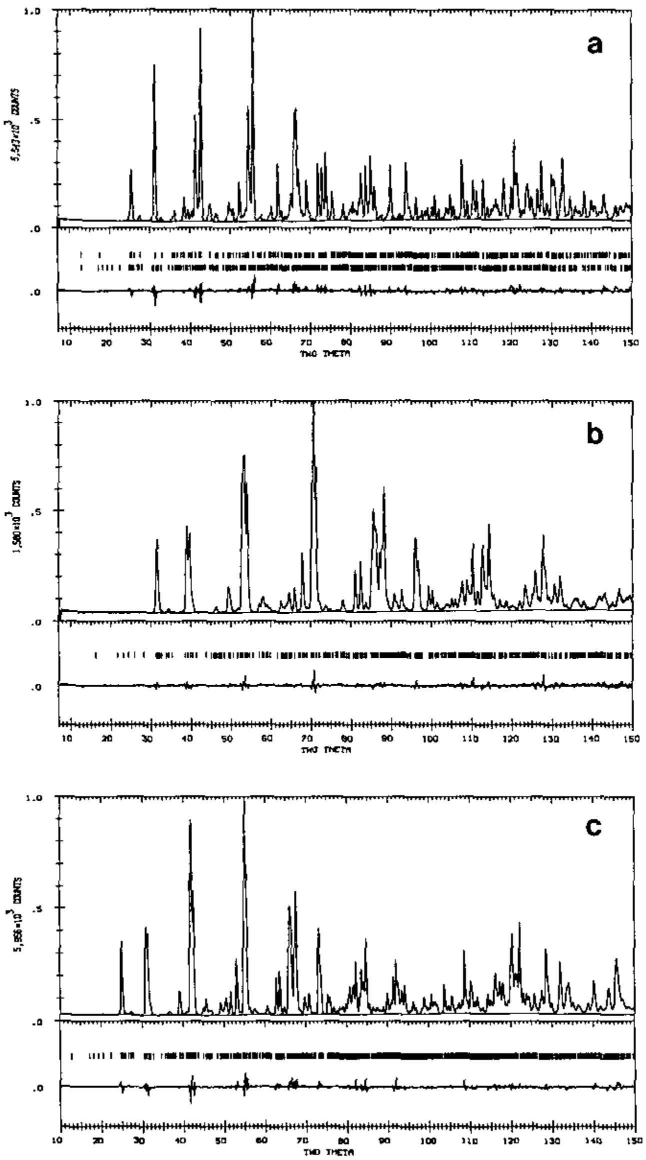

FIG. 1. Observed, calculated, and difference intensities of neutron powder patterns for (a) orthorhombic $CuNb_2O_6$ (upper bars) with some impurities of monoclinic $CuNb_2O_6$ (lower bars), (b) monoclinic $CuNb_2O_6$, and (c) $Cu_{0.85}Zn_{0.15}Nb_2O_6$.

verge with correlated parameters at values which are not shifted more than 1.4% ($P2_1$) or 16% ($P\bar{1}$) of their estimated standard deviations. Whereas the assumption of $P\bar{1}$ results in an increased isotropic temperature factor B for Cu with respect to that of Nb, the refinement with $P2_1$ leads to an increased B for Nb. Variation of the molar ratios of copper and niobium on the Cu and Nb sites converged to the unmixed distribution. Therefore, a partial occupation of niobium sites by copper is improbable.

The parameters of the crystal structure of orthorhombic $CuNb_2O_6$, which result from X-ray single-crystal data, are given in Table 3; they agree with previously published values (7, 16, 17) and with a refinement of the well-resolved neutron powder diffraction data collected at D2B. An impurity, which consisted of about 10% monoclinic $CuNb_2O_6$, had to be taken into account (see Fig. 1a). A projection of the copper planes is shown in Fig. 2a.

The crystal structure of monoclinic $Cu_{0.85}Zn_{0.15}Nb_2O_6$ features identical structural details as monoclinic $CuNb_2O_6$ (see Table 3 and Fig. 2b): A projection onto the ac plane for atoms within $-0.2 \leq y \leq 0.2$ shows the zigzag chains of edge-sharing CuO_6 octahedra (see Fig. 2b). These octahedra are tetragonally elongated due to the Jahn–Teller effect and aligned along a vector

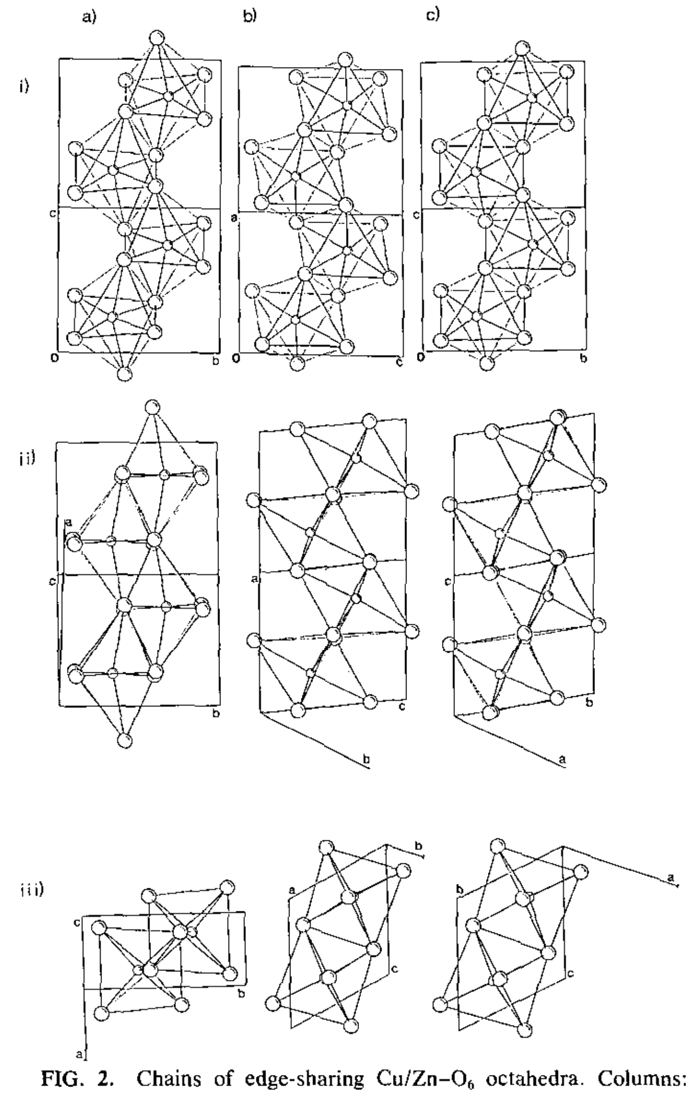

FIG. 2. Chains of edge-sharing Cu/Zn–O_6 octahedra. Columns: (a) orthorhombic $CuNb_2O_6$; (b) monoclinic $CuNb_2O_6$ and $Cu_{0.85}Zn_{0.15}Nb_2O_6$; and (c) orthorhombic $Cu_{0.36}Zn_{0.64}Nb_2O_6$. Lines: (i) projections on the bc ($Pbcn$) and ca plane ($P2_1/c$), respectively; (ii) view perpendicular to the elongated O–Cu–O bondings; and (iii) view along the elongated O–Cu–O bondings.

TABLE 3
Refined Atomic Coordinates and Temperature Factors of Orthorhombic and Monoclinic $CuNb_2O_6$, $Cu_{0.85}Zn_{0.15}Nb_2O_6$, and $Cu_{0.36}Zn_{0.64}Nb_2O_6$

	Orthorhombic $CuNb_2O_6$		Monoclinic $CuNb_2O_6$		$Cu_{0.85}Zn_{0.15}Nb_2O_6$		$Cu_{0.36}Zn_{0.64}Nb_2O_6$	
	x, y, z	$u_{11}, u_{22}, u_{33}, u_{23}, u_{13}, u_{12}$ (10^{-}Å^2)	x, y, z	B(Å)	x, y, z	B(Å)	x, y, z	$u_{11}, u_{22}, u_{33}, u_{23}, u_{13}, u_{12}$ (10^{-}Å^2)
Cu (Zn)	0.0	72(2)	0.2502(7)	0.58(5)	0.2518(5)	0.53(4)	0.0	65(3)
	0.3297(1)	62(2)	0.0002(3)		0.0011(2)		0.3272(1)	83(3)
	0.25	85(3)	0.3420(5)		0.3383(4)		0.25	75(3)
		0						0
		21(2)					occ.(Cu): 0.36(8)	−2(2)
		0						0
Nb1	0.1598(0)	59(1)	0.7370(6)	0.19(5)	0.7371(4)	0.33(4)	0.3396(0)	48(2)
	0.1825(0)	61(1)	0.1607(2)		0.1599(2)		0.3180(1)	42(2)
	0.7805(0)	45(1)	0.2037(4)		0.2014(3)		0.2444(1)	53(2)
		1(1)						1(1)
		−3(1)						3(1)
		0(1)						1(1)
Nb1a			0.2353(6)	0.25(6)	0.2336(4)	0.19(4)		
			0.1615(2)		0.1623(2)			
			0.8466(4)		0.8411(4)			
O1	0.0922(2)	83(9)	0.0627(8)	0.33(7)	0.0621(6)	0.32(5)	0.0962(2)	68(9)
	0.1024(4)	74(8)	0.0965(3)		0.0963(2)		0.1047(4)	61(9)
	0.1006(4)	56(10)	0.1378(6)		0.1321(5)		0.0673(5)	64(10)
		7(8)						2(8)
		4(7)						12(8)
		12(7)						15(8)
O1a			0.5737(9)	0.47(8)	0.5759(7)	0.42(4)		
			0.0781(3)		0.0784(2)			
			0.4009(6)		0.3991(5)			
O2	0.4161(2)	99(9)	0.4037(8)	0.29(7)	0.4049(6)	0.44(4)	0.2443(2)	71(9)
	0.0955(4)	88(9)	0.2451(2)		0.2448(2)		0.1222(4)	60(9)
	0.1459(5)	101(11)	0.1448(4)		0.1430(4)		0.4144(5)	60(10)
		0(9)						9(8)
		−4(8)						10(9)
		24(7)						−9(8)
O2a			0.9002(9)	0.47(7)	0.9008(6)	0.55(4)		
			0.2448(3)		0.2448(2)			
			0.9086(5)		0.9040(4)			
O3	0.7589(2)	78(8)	0.5560(9)	0.54(8)	0.5560(6)	0.50(4)	0.4198(2)	86(10)
	0.1282(4)	83(8)	0.0969(3)		0.0974(2)		0.1188(4)	64(9)
	0.0474(4)	62(9)	0.9229(6)		0.9212(5)		0.0866(5)	91(11)
		8(8)						−15(9)
		7(7)						16(9)
		23(7)						20(8)
O3a			0.0643(9)	0.69(8)	0.0643(7)	0.58(4)		
			0.0799(3)		0.0795(2)			
			0.6519(6)		0.6489(5)			

(−0.620, 0.177, 0.547), i.e., along [−3 12 4]. In contrast to this configuration, the long O–Cu–O axes in orthorhombic $CuNb_2O_6$, drawn in an analogous projection, lie parallel to [6 0 1] [remember the interchange of the axes, if the symmetry is increased ($P2_1/c \rightarrow Pbcn$): $a_{mon} = c_{orth}$, $b_{mon} = a_{orth}$, $c_{mon} = b_{orth}$] (see Fig. 2a). Besides the orientation of the long axes of the octahedra, there are differences in the Cu–O distances: The two elongated Cu–O bonds have the identical length in orthorhombic $CuNb_2O_6$ (238 pm), while they are shortened and different in monoclinic $CuNb_2O_6$ (229 and 233 pm, respectively). The intrachain Cu–Cu distances are 320 pm in orthorhombic $CuNb_2O_6$, while they alternate in monoclinic $CuNb_2O_6$ between 305 and 314 pm. This may influence magnetic ordering phenomena.

The crystal structure of $Cu_{0.36}Zn_{0.64}Nb_2O_6$, see Table 3 and Fig. 2c, resembles that of $ZnNb_2O_6$ (8), but not that of monoclinic or orthorhombic $CuNb_2O_6$. In $ZnNb_2O_6$ and $Cu_{0.36}Zn_{0.64}Nb_2O_6$, no long O–Cu/Zn–O axes are detectable by diffraction methods. Still, two slightly elongated Cu/Zn–O distances are observed in the octahedron (218 pm), but these bonds are almost perpendicular to each other. Studies of the *X*-ray *a*bsorption *n*ear-*e*dge *s*tructure (XANES) at the Cu-K edge show similar surroundings of copper for all mixed oxides and for monoclinic $CuNb_2O_6$, whereas a different coordination sphere is formed in orthorhombic $CuNb_2O_6$ (9, 16). Therefore the monoclinic distortion, which increases with the copper content, may be caused by statistically distributed elongated CuO_6 octahedra, which are oriented in the same manner. The other orientation found in orthorhombic $CuNb_2O_6$ allows the system to achieve a higher symmetry.

2. *Phase Transitions of $CuNb_2O_6$*

DTA–TG curves of monoclinic and orthorhombic $CuNb_2O_6$ are plotted in Fig. 3. By heating, both modifications of $CuNb_2O_6$ are partially reduced in two steps: At a temperature of 977°C for monoclinic and 1004°C for orthorhombic $CuNb_2O_6$, a slightly endothermic oxygen loss of 0.05(1)% of the formula mass occurs (estimated errors in parentheses). When both samples of $CuNb_2O_6$ melt at 1143°C, they take a second step and lose 1.1(1)% of their total mass. Both steps are reverted when the samples resolidify. The solidified melt of monoclinic $CuNb_2O_6$, however, was found to consist of single-phase orthorhombic $CuNb_2O_6$ as determined by X-ray diffractometry. The stoichiometries, which correspond to the products of the reductions, are $CuNb_2O_{5.99}$ for the first step and $CuNb_2O_{5.75}$ for the second step, if a full stoichiometry is assumed for the starting products monoclinic and orthorhombic $CuNb_2O_6$ at room temperature. An-

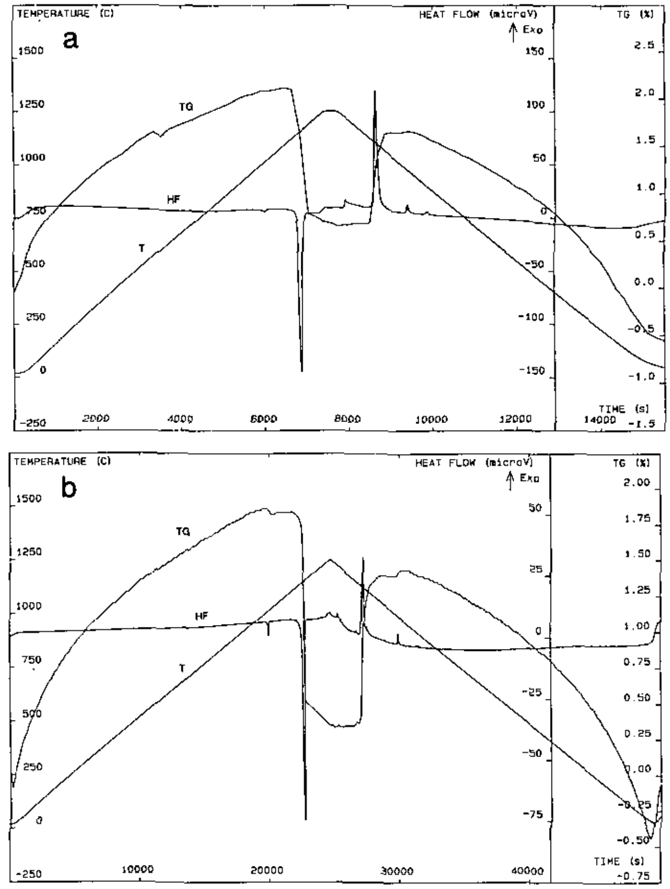

FIG. 3. DTA–TG analyses of (a) monoclinic and (b) orthorhombic $CuNb_2O_6$ under an O_2 atmosphere.

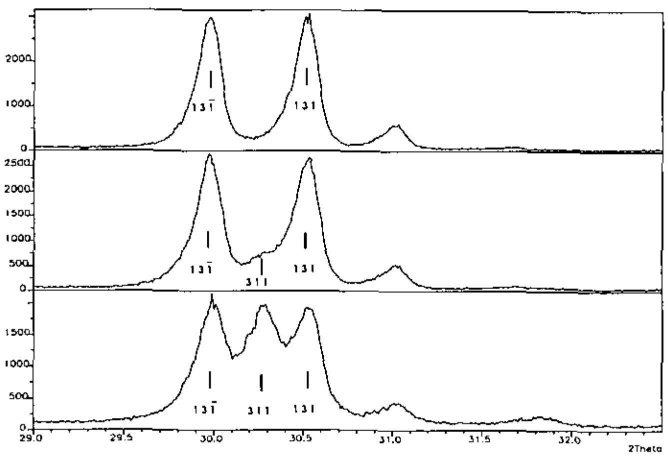

FIG. 4. The 1 3 $\bar{1}$ and 1 3 1 reflections of monoclinic and 3 1 1 reflection of orthorhombic $CuNb_2O_6$: (a) sieved, unground grains of single-phase monoclinic $CuNb_2O_6$ with a diameter of less than 56 μm; (b) the same sample, ground in an agate mortar; and (c) thoroughly ground monoclinic $CuNb_2O_6$. Small shifts of the peak positions are caused by slightly disadjusted samples.

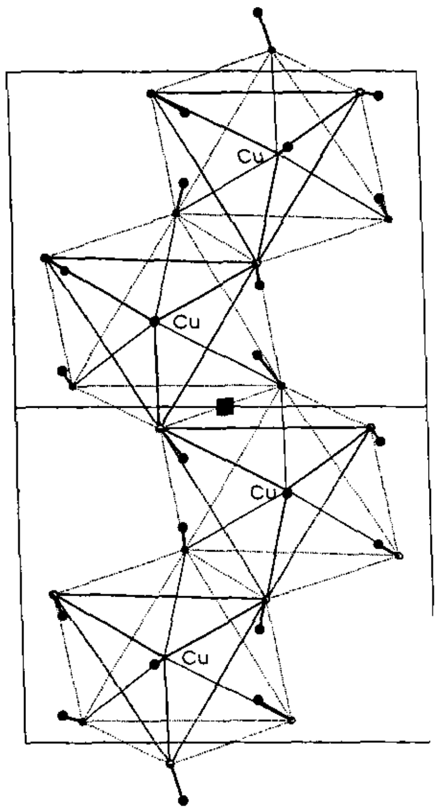

FIG. 5. Cu–O_6 octahedra of monoclinic $CuNb_2O_6$, projected onto the *ca* plane. Black points show the atom positions after the transition to orthorhombic $CuNb_2O_6$. The black square marks the arbitrarily chosen point of congruence of both cells.

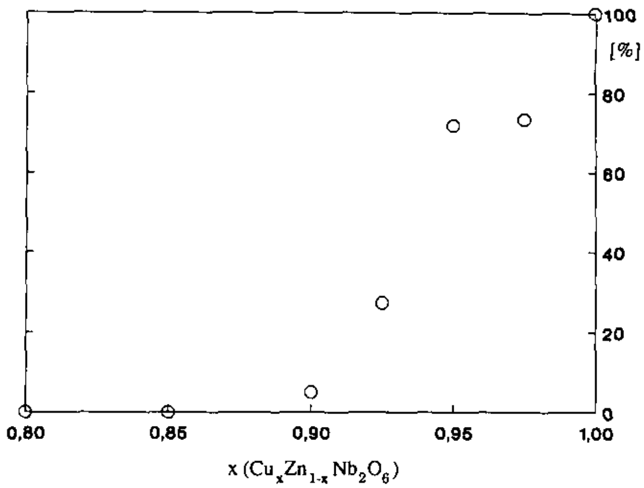

FIG. 7. Contents of the orthorhombic phase in a mixture of orthorhombic and monoclinic $Cu_xZn_{1-x}Nb_2O_6$.

other exothermic transition is observed for both samples at about 920°C, while the sample is cooled.

Monoclinic $CuNb_2O_6$ undergoes a stress-induced phase transition to orthorhombic $CuNb_2O_6$. This follows from observations of ground samples of single-phase monoclinic $CuNb_2O_6$. Figure 4 displays powder diffraction patterns of three samples of monoclinic $CuNb_2O_6$ which have been ground with different intensities. Reversibility of this process was not observed. The transformation from monoclinic to orthorhombic $CuNb_2O_6$ by grinding may be explained on a microscopic scale. It is possible to transform monoclinic $CuNb_2O_6$ to its orthorhombic modification, if the oxygen layers above and below a copper layer glide along [1 0 1] (in $P2_1/c$) in opposite directions and if the chains of CuO_6 octahedra are stretched simultaneously in their direction of propagation (see Fig. 5); i.e., the nature of the transition from monoclinic to orthorhombic $CuNb_2O_6$ is displacive. Additionally, there exists a group–subgroup relation ($Pbcn \rightarrow P2_1/c$: *t*2). The observed transition is accompanied by a 0.8% volume reduction of the unit cell. A retransformation from orthorhombic to monoclinic $CuNb_2O_6$ was not observed despite some experimental efforts. Therefore, mono-

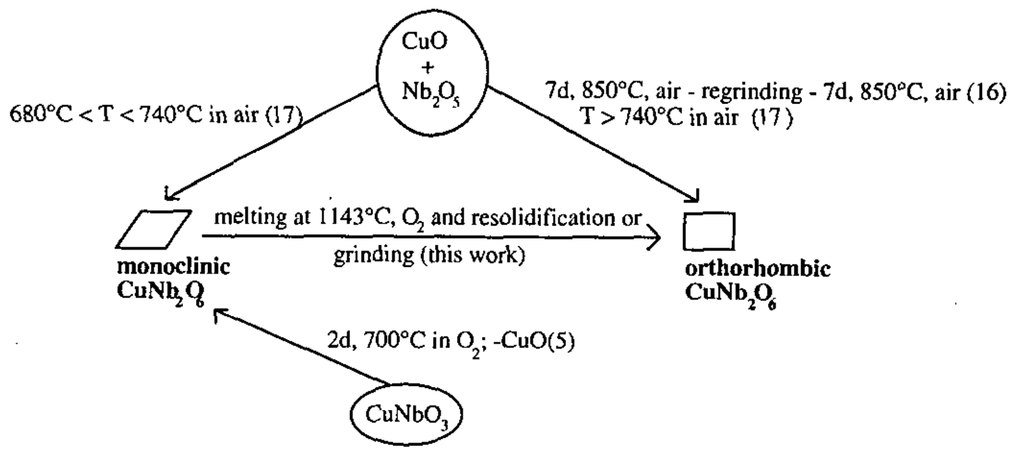

FIG. 6. Summary of chemical reactions and transformations yielding monoclinic and orthorhombic $CuNb_2O_6$.

clinic $CuNb_2O_6$ seems to be less stable at room temperature than orthorhombic $CuNb_2O_6$. Chemical reactions and phase transitions, which yield monoclinic and orthorhombic $CuNb_2O_6$, are summarized schematically in Fig. 6. The monoclinic structure is stabilized by substituting copper by zinc. The preparation of mixed oxides $Cu_xZn_{1-x}Nb_2O_6$, with $0.9 \leq x < 1$, under conditions described under Experimental Details yields monoclinic and orthorhombic phases simultaneously in the proportions displayed in Fig. 7 [see (16)]. The decreasing content of the orthorhombic phase with decreasing copper content is an argument for a miscibility gap. There is obviously a maximal copper content of $x \approx 0.9$, below which the monoclinic structure is the stable phase. Recent temperature-dependent X-ray powder diffraction experiments confirm this assumption.

ACKNOWLEDGMENTS

Support of this work by Deutsche Forschungsgemeinschaft Project We 1542/2-1 and the Bundesministerium für Forschung und Technologie is gratefully acknowledged. Thanks are due to the Institut Laue Langevin in Grenoble and the Laboratoire Commun CEA-CNRS, Laboratoire Léon Brillouin, Saclay, for the provision of beam time at D2B and D1A.

REFERENCES

1. H. J. Sturdivant, *Z. Kristallogr.* **75,** 88 (1930).
2. H. Weitzel, *Z. Kristallogr.* **144,** 238 (1976).
3. E. J. Felten, *J. Inorg. Nucl. Chem.* **29,** 1168 (1967).
4. H. Kasper, *Rev. Chim. Miner.* **4,** 759 (1967).
5. E. Wahlstroem and B. O. Marinder, *Inorg. Nucl. Chem. Lett.* **13,** 559 (1977).
6. V. Propach and D. Reinen, *Z. Anorg. Allg. Chem.* **369,** 278 (1969).
7. H. Weitzel, *Kernforschungszent. Karlsruhe Ber., KfK* **3381,** 114 (1982).
8. M. Waburg and H. Müller-Buschbaum, *Z. Anorg. Allg. Chem.* **508,** 55 (1984).
9. J. Norwig, H. Weitzel, and H. Fuess, *Fresenius J. Anal. Chem.,* **339,** 152 (1994).
10. G. M. Sheldrick, SHELX-76: Program for Crystal Structure Determination. Cambridge, UK, 1976.
11. G. M. Sheldrick, SHELXS-86: Program for Crystal Structure Solution. Göttingen, 1986.
12. R. J. Hill and C. J. Howard, LHPM1: A Computer Program for Rietveld Analysis of Fixed Wavelength X-Ray and Neutron Powder Diffraction Patterns. Australian Atomic Energy Commission, Research Establishment, 1986.
13. D. B. Wiles and R. A. Young, *J. Appl. Crystallogr.* **14,** 149 (1981).
14. H. M. Rietveld, *J. Appl. Crystallogr.* **2,** 65 (1969).
15. C. J. Howard, *J. Appl. Crystallogr.* **15,** 615 (1982).
16. J. Norwig, Diploma thesis, Fachbereich Chemie, TH Darmstadt, 1992.
17. B. Kratzheller and R. Gruehn, *J. Alloys Compounds* **183,** 75 (1992).